

DETERMINATION AND EVALUATION OF RESIDUAL STRESSES IN THICK-WALLED CYLINDERS DUE TO AUTOFRETTAGE

H.J. Schindler ¹, P. Bertschinger¹, C.H. Nguyen ¹, R. Knobel ²

¹ Swiss Federal Laboratories for Materials Testing and Research (EMPA), Dübendorf, Switzerland; ² Swiss Ordnance Enterprise (SW), Thun, Switzerland

ABSTRACT

Autofrettage is a treatment to introduce beneficial residual stresses into thick-walled cylinders to improve their performance under repeated loading by internal pressure. In the present investigation the residual stresses are measured and their effect was analysed and discussed. The experimental determination of the residual stress distribution was performed by the crack-compliance-method. The corresponding influence function for thick-walled cylinders, which is needed for the experimental stress measurement by the CC-method, was derived analytically. Besides the residual stresses this method enables one to obtain also the stress-intensity factor as a function of cut depth, which is required in the theoretical fatigue life prediction based on linear-elastic fracture mechanics. Examples of experimental data are presented. To validate the experimental results they are compared with analytical calculations. The agreement between the calculated and measured residual stresses was satisfying. Furthermore the effect of the axial dimension (plane-stress vs. plane strain), which has to be taken into account when using a thin disk for stress measurement by the CC-method, is investigated by a 3D FEM-analysis.

INTRODUCTION

Autofrettage is a well-known and efficient method to introduce beneficial residual stresses in thick-walled cylinders which are loaded in service by internal pressure. Essentially, the treatment consists of an overload by internal pressure such that a major part of the cylinder wall is plastically deformed. After unloading, compressive stresses remain near the inner surface. These stresses are able to prevent or at least retard fatigue crack growth and stress corrosion cracking. Thus, knowledge of the residual stresses is essential to assess the safety and to predict the remaining life of a pipe loaded repeatedly by internal pressure.

The aim of the present investigation was to determine and evaluate the residual stresses in a thick-walled cylinder of 125 mm outer diameter and a length of about 5 m. It was treated by autofrettage several years ago and has been since then in service as a gun-barrel, loaded by hundreds of relatively large load cycles. One of the questions was to what degree the initial residual stresses are still present, since an unknown portion of them is expected to be faded away during service. The original treatment was not known exactly either, so another aim was to get information about the initial pressure and the corresponding initial residual stresses. Regarding these aims, a straightforward measurement technique is the crack- (or cut-) compliance method (CC-method). Its principle is described in [1 – 5] and further

literature given therein. In the present paper the application of the CC-method to the case of a thick-walled cylinder is shown and discussed. The scientific challenge of this task was the large size of the test piece, which made prior sectioning necessary, and the geometry, which was new for the CC-method. Since the residual stresses due to autofrettage can be calculated analytically, these tests also offered the possibility to validate the method by comparison between measured and calculated stresses.

MEASUREMENT OBJECT AND PROCEDURE

The cylinder in question has an inner and outer radius of $r_i=65\text{mm}$ and $r_a=125\text{ mm}$, respectively, and a length of about 5m. The material is 35 NiCrMoV 12 5 quenched and tempered steel with a yield stress of $R_p = 898\text{ N/mm}^2$ and an ultimate tensile strength of $R_m = 988\text{ N/mm}^2$. The cylinder was in service for several years, loaded by several hundreds of load cycles of about 4000 bar (i.e. 400 N/mm^2). As reported, the pressure of the autofrettage process was chosen such that about two thirds of the cylinder wall thickness should be plastically deformed, while the outer third remained in the elastic state. As shown later, this corresponds theoretically to a pressure of about 6000 bar.

As described in detail in [1-5] the CC-method requires a progressive cut to be introduced along the plane where the residual stresses are to be measured. The main residual stresses due to autofrettage are tangential stresses $\sigma_\varphi(x)$, which require cutting in a radial-axial plane. To enable local radial cutting a relatively thin ring-shaped slice (Fig. 1a) has to be cut off the pipe by two cuts perpendicular to the axis. In the present case a thickness of 43 mm was chosen. Thereby the major part of the axial residual stresses is released, which also affects the tangential residual stresses that are to be determined. This effect has to be accounted for.

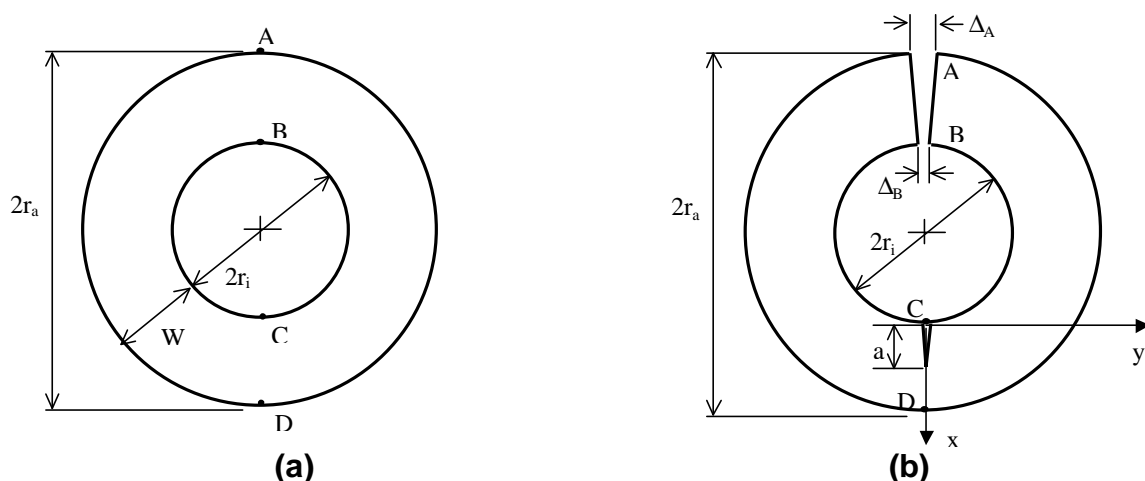


Fig. 1: Ring as cut from the pipe (a) and in the open state (b) (after cutting the section A – B)

To apply the CC-method to the ring as shown in Fig. 1a it is advantageous to separate it first by a cut on section A – B such that an open ring as shown in Fig. 1b results. The advantage is twofold: First, the strain change in the vicinity of section C-D is more significant, thus the measurement is more sensitive, and second, the

influence function can be relatively easily estimated on the basis of existing solutions, as shown in the next section. However, by the prior cut of section A – B, a certain portion of the residual stresses in the cross-section C – D is released and must be accounted for afterwards. As shown in the next section, the corresponding portion of the residual stresses can be quantified from measurements of the cut opening displacement at A and B, or by strain measurements at C or D.

Since the accuracy of the CC-method is better in the range of short and medium cut depths, and the residual stresses at the inner part of the wall were of greater interest than those on the outer part, it is preferable to introduce the cut from the inside, along the x –axis as shown in Fig. 1b. The strain was measured by two strain gages, one on the inner surface in a distance of 6 mm from C and the other on the outer surface at D. According to the principle of the CC-method [1 - 5] the stress intensity factor (SIF) due to the residual stresses acting at the cut front, $K_{irs}(a)$, is obtained by

$$K_{irs}(a) = \frac{E'}{Z(a)} \frac{d\varepsilon_M}{da} \quad (1)$$

where a is the actual cut depth, ε_M is the strain measured by the above-mentioned strain gages, and Z the influence function. For the strain gage near C the function $Z(a)$ given in [4, 5] for a short edge cut in a rectangular plate can be used with sufficient accuracy for $a \ll r_i$. For the strain gage at D the Z -function was not available, so it was estimated from known functions in related systems (see next section). From $K_{irs}(a)$ the residual stress distribution $\sigma_{rs}(x)$ can be calculated as described in [2, 5, 6] by inversion of the equation

$$K_{irs}(a) = \int_0^a h(x, a) \cdot \sigma_{rs}(x) \cdot dx \quad (2)$$

Here $h(x, a)$ denotes the weight function as introduced by Bueckner [7].

ANALYTICAL CONSIDERATIONS

Influence function. $Z(a)$ for the strain gage at location D can be obtained as an approximation relatively easily by combining the influence function for a disk and the one for a rectangular plate. Recalling that the physical meaning of Z is the strain change at D per unit cut extension and unit of K_i , it is obvious that for $r_i \ll W$ it tends towards $Z(a' = W + 2r_i + a)$ of a circular disk as given in [4, 5], whereas for $W \ll r_a$ it tends towards $Z(a)$ for a rectangular plate, which also is given in [4, 5]. Without going into the details of the corresponding mathematics, matching of these two solutions leads to

$$Z(a) = 1.7897 \cdot \sqrt{\frac{2r - 1 + a/W}{r(W - a)^3}} \quad \text{for } a/W > 0.2(\rho - 1)/\rho \quad (3a)$$

$$Z(a) = \frac{B}{(W - a)^{3/2}} \cdot \sqrt{1 - \left(\frac{a/W - A}{A}\right)^2} \quad \text{for } a/W < 0.2(\rho - 1)/\rho \quad (3b)$$

where

$$A = \frac{y_0 x_0 - s x_0^2}{y_0 - 2s x_0} \quad B = \frac{y_0}{\sqrt{1 - \left(\frac{a/W - A}{A}\right)^2}} \quad s = 0.8949 \cdot \sqrt{\frac{\mathbf{r}}{2\mathbf{r} - 1 + \frac{0.2(\mathbf{r} - 1)}{\mathbf{r}}}}$$

$$\rho = r_a/W \quad x_0 = 0.2(\rho - 1)/\rho \quad ; \quad y_0 = Z(a = x_0 W) \cdot W^{3/2} (1 - x_0)^{3/2}$$

The functions (3a) and (3b) are shown graphically in Fig. 2.

Stress release due to prior cutting. Prior cutting at section A-B releases the corresponding residual stresses. Because of the condition of axial symmetry of the stresses, the resultant of the released stresses is a pure bending moment M acting on both sides of section A – B and affecting correspondingly the residual stresses in section C - D. According to [8] the tangential stresses in section C – D due to a bending moment M are

$$\mathbf{s}_{jB} = -\frac{4M}{N} \left(-\frac{r_i^2 \cdot r_a^2}{\mathbf{r}^2} \ln \frac{r_a}{r_i} + r_a^2 \cdot \ln \frac{\mathbf{r}}{r_a} + r_i^2 \cdot \ln \frac{r_i}{\mathbf{r}} - r_i^2 \right) \quad (4a)$$

where

$$N = (r_a^2 - r_i^2)^2 - 4r_a^2 \cdot r_i^2 \cdot \left(\ln \frac{r_a}{r_i} \right)^2 \quad (4b)$$

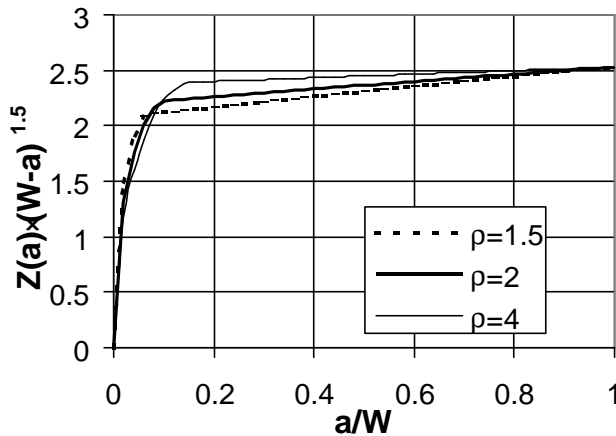


Fig. 2: $Z(a)$ for cylinders for some values of $\rho = r_a/W$

By (4) and a single strain measurement at an arbitrary location x the stress distribution in cross-section C-D due to the stress release on section A-B can be determined. Another, independent possibility to account for this global bending effect due to M is by measuring the cut opening displacements at A and B, Δ_A and Δ_B . The required relation between the stress on C-D and the cut opening displacement can be easily established by the theory of curved beam bending according to [8]. One finds:

$$\Delta_A - 0.394\Delta_B = \frac{1.65 \cdot \mathbf{P}}{E \cdot W} (R_i + 0.606W)^2 \cdot \mathbf{s}_{jB}(x = 0) \quad (5)$$

Effect of plane stress. When a relatively thin slice is cut off a long cylinder, the state of residual stresses changes from tri-axial to essentially plane stress, which affects the tangential residual stress. Since autofrettage causes plastic deformation under plane strain conditions, the axial stresses after unloading are about $\sigma_a = \nu \cdot \sigma_\phi$ (with ν

being Poisson's ratio). Due to cutting perpendicular to the axis, these stresses are released. This is accompanied by a relaxation of the residual tangential stresses by the amount of $\nu \cdot \sigma_a = \nu^2 \cdot \sigma_\phi$, which has to be added to the residual stresses measured in the slice.

Combining the above-discussed effects the initial residual stress is obtained as

$$\sigma_{rs/pipe}(x) = (1+\nu^2) \cdot (\sigma_{rs}(x) + \sigma_{\phi b}(x)) \quad (6)$$

EXPERIMENTAL DATA

The above defined deformation parameters measured after cutting section A – B were as follows:

- cut opening displacement: $\Delta_A = 1.5 \text{ mm}; \quad \Delta_B = 0.9 \text{ mm}$ (7a)
- global bending strain at D: $\varepsilon_{Db} = 0.000504$ (7b)

By (4) or (5), respectively, the corresponding stress distribution on section C – D can be calculated from either (7a) or (7b). The agreement is better than 10%, thus confirming each other. Being more directly related to the stress, the strain ε_{D0} is used for the stress distribution to be determined. Eq. (4), (7b) and Hooke's law results in

$$M = 3.32 \text{ Nm} \quad (8)$$

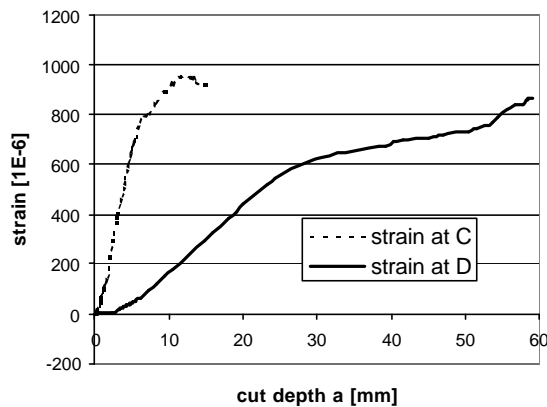


Fig. 3: Strain measured at C and D as a function of cut depth a

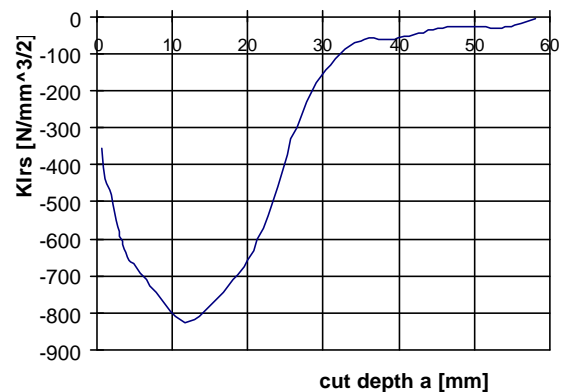


Fig. 4: Stress intensity factor calculated by (1) from curves shown in Fig. 3.

Fig. 3 shows the strain change due to progressive cutting along the x-axis measured by the strain gages at C and D as a function of cut depth. Generally, the higher the slope of these curves, the better the sensitivity of the corresponding measurement location. Accordingly, as expected, the strain gage near C is sensitive in the range of about $a < 10 \text{ mm}$, and the one at D for about $a > 5 \text{ mm}$. The SIF obtained by (1) from these two strain measurements by (1) is shown in Fig. 4, where for $a < 4 \text{ mm}$ the influence function $Z(a)$ for a short crack in a rectangular plate was used, and for $a > 6 \text{ mm}$ eqs. (3a) and (3b). In the intermediate range, these two curves were matched such that a smooth transition occurs. From the curve shown in Fig. 4 the

residual stress distribution $\sigma_{rs}(x)$ was calculated by using (2). Lacking the weight function $h(x,a)$ for this crack configuration, the one for a rectangular plate was used as an approximation. This is justified by the fact that the latter holds for short cracks (i.e. $a \ll r_i$) as well as for deep cracks (i.e. $(W-a) \ll W$), so it is expected to be sufficiently accurate even in the intermediate range of crack depths. The resulting curve is shown in Fig. 5. The total residual stress in the pipe, which also is shown in Fig. 5, is calculated by (6), using (4) and (8) to account for the global bending effect.

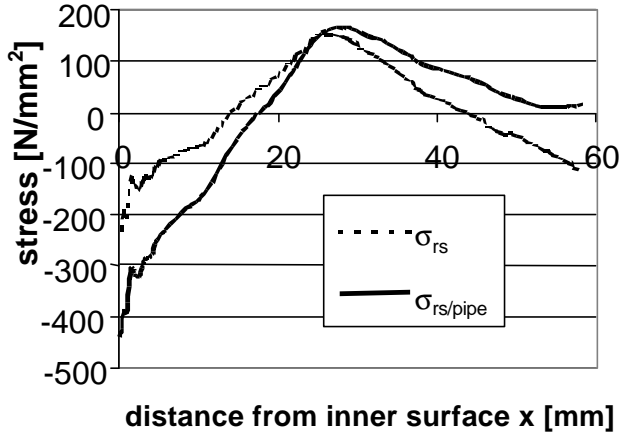


Fig. 5: Residual stress in open ring and total tangential residual stress in the pipe

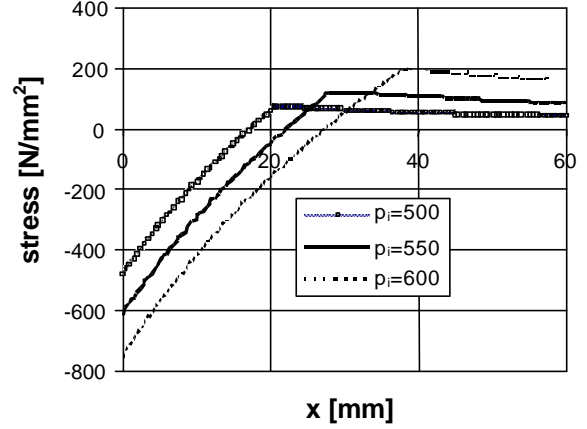


Fig. 6: Residual stresses analytically calculated for three values of internal pressure p_i (in N/mm^2)

ANALYTICAL CALCULATION OF RESIDUAL STRESSES

In order to validate the experimental procedure the measured stresses are compared with those analytically and numerically calculated. The analytical determination of residual stresses due to autofrettage is rather simple. According to [8] the elastic tangential stresses in a cylinder (Fig. 1a) due to internal pressure p_i are

$$\mathbf{s}_j(x) = \frac{R_i \cdot p_i}{R_a^2 - R_i^2} \cdot \left(1 + \frac{R_a^2}{(R_i + x)^2} \right) \quad (9)$$

In the region where Tresca's yield criterion $\sigma_\phi(x) - \sigma_r(x) < R_p$ is violated, $\sigma_\phi(x)$ is obtained from

$$\sigma_\phi(x) = R_p + \sigma_r(x) \quad (10)$$

where the radial stress $\sigma_r(x)$ is obtained from the equilibrium and yield condition, which lead to the integral equation

$$\mathbf{s}_r(x) = \frac{-R_i}{R_i + x} \cdot p_i + R_p \cdot \ln \frac{R_i + x}{R_i} - \int_0^x \frac{\mathbf{s}_r(x)}{R_i + x} dx \quad (11)$$

The residual stress distribution is obtained by (10), the numerical solution of (11) and subtracting the elastic stresses (9) due to unloading. For the present geometry of the

pipe and elastic-perfectly plastic material with a yield stress of $R_p = 900 \text{ N/mm}^2$ the resulting curves are shown in Fig. 6 for some values of internal pressure.

Effect of plane stress. To verify the correction made in (6) to account for plane stress, a 3D- finite element stress calculation was carried out. The axial residual stresses under plane stress turned out to be about $\sigma_a = \nu \cdot \sigma_\phi$ near the inner surface, and about $\sigma_a = \nu \cdot \sigma_\phi / 2$ near the outer surface. As predicted by the above theoretical considerations the residual stresses in the ring are about 10% lower than the ones under plane strain.

DISCUSSION

Comparison with analytical solution. Qualitatively, the agreement between measured and calculated residual stress is good, indicating that there is no fundamental error in the measurement method. Quantitatively an agreement better than about 10 - 20% is not to be expected for the following reasons: i) The material is not elastic-perfectly plastic. ii) Tresca's yield criterion is an approximation of the real yield behaviour. iii) After autofrettage, a material layer of some millimetres thickness was removed from the inner surface. Moreover, as discussed above, the weight function used is only an approximation.

As can be seen from the analytical solution, the location of the maximum tensile residual stress corresponds to the original elastic-plastic boundary. Thus, from comparison of Fig. 5 and 6 one can conclude that the pressure used for autofrettage was about 550 N/mm^2 in the present case, thus lower than the two third plastic deformation that the treatment aimed at. Therefrom one can estimate the initial residual stress after autofrettage by the corresponding curve shown in Fig. 6, which is about -600 N/mm^2 at the inner surface. Compared with the measured values, one can conclude that about one third of the initial residual stresses are relaxed due to the service loads.

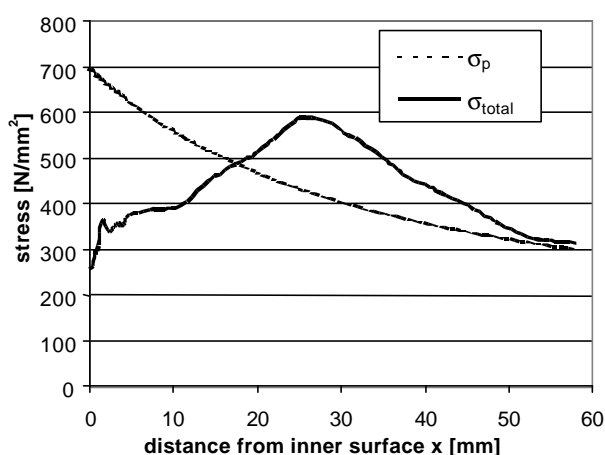


Fig. 7: Comparison of tangential stress due to the service load of $p=400 \text{ N/mm}^2$ with (σ_{total}) and without (σ_p) measured residual stresses

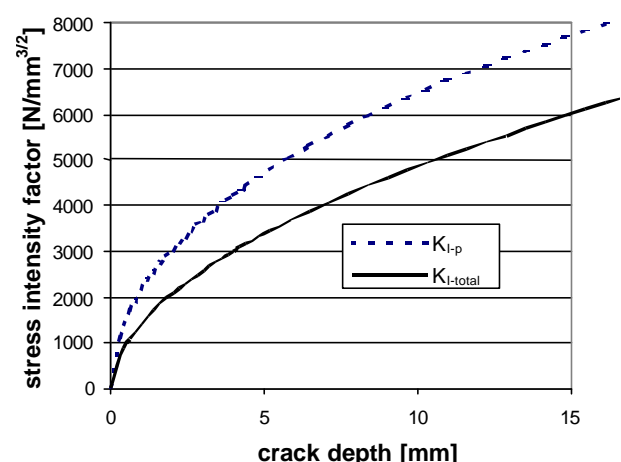


Fig. 8: Comparison of SIF due to internal pressure $p=400 \text{ N/mm}^2$ with ($K_{I\text{-total}}$) and without ($K_{I\text{-p}}$) residual stresses

Effect of residual stresses. Fig. 7 shows the comparison of the tangential stresses due to the service load of $p=400 \text{ N/mm}^2$ with and without the measured residual stresses. Therefrom one can see that the measured residual stresses reduce the maximum tensile stresses near the inner surface, which is crucial for subcritical crack initiation, by more than 50%. The reduction effect of the residual stresses on the SIF of an eventual surface crack is not quite as significant, but still about 33% (Fig. 8). Concerning eventual fatigue crack growth, this reduction results in a retardation of the crack growth rate by about 80%, because according to Paris' law the growth rate depends on the SIF by about the 4th power. Furthermore, as can be seen from Fig. 8, the critical crack size (i.e. the crack depth at the level of fracture toughness, which for the present material is estimated to be about $K_{Ic}=4000 \text{ N/mm}^{3/2}$) is about twice the one without residual stresses.

CONCLUSIONS

Concerning the method of residual stress determination:

- The CC-method is applicable to measure residual stresses in large pipes
- The weight function for a rectangular plate can be used as an approximation, however, a more exact weight function should be determined to improve the accuracy.

Concerning the physical effects of the residual stresses:

- The majority (about 2/3) of the residual stresses introduced by autofrettage are still present after several years of service.
- They reduce the operating stress at the inner surface by more than 50%
- They reduce the SIF by more than 30%, which corresponds to a retardation of the fatigue growth rate by about 80%.
- The critical crack size is extended by about 100%.
- Due to the reduced crack growth rate, the inspection intervals can be prolonged.

References:

- [1] Cheng, W., Finnie, I., ASME J. of Eng. Mat. and Tech., Vol 108, 87-92 (1986)
- [2] Prime, M.B., Appl. Mech. Reviews, Vol. 52, No. 2 (1999), 75-96
- [3] Schindler, H.J., Cheng, W., Finnie, I., J. Experimental Mechanics, Vol. 37, No. 3 (1997) 272-279
- [4] Schindler, H.J. and Landolt R., Proc. of 4th Europ. Conf. on Residual Stresses, Cluny (F) (1996) 509 - 518
- [5] Schindler, H.J., Bertschinger, P. Proc. 5th Int. Conf. on Residual Stresses, Linköping, Sweden, 1997, Ed. T. Ericson, et al., Vol. 2, 682-687
- [6] Schindler, H.J., Int. J. Fracture, Vol. 74, (1995) R23-R30,
- [7] Bückner, H., Zeitschrift für angew. Mathematik und Mechanik (ZAMM), 50 (1970) 529-545
- [8] S.P. Timoshenko, J.N. Goodier, Theory of Elasticity, McGraw-Hill, 3rd Ed., (1970)